Learning Activation Functions for Sparse Neural Networks

Anonymous[1]

[1]Anonymous Institution

Abstract Sparse Neural Networks (SNNs) can potentially demonstrate similar performance to their dense counterparts while saving significant energy and memory at inference. However, the accuracy drop incurred by SNNs, especially at high pruning ratios, can be an issue in critical deployment conditions. While recent works mitigate this issue through sophisticated pruning techniques, we shift our focus to an overlooked factor: hyperparameters and activation functions. Our analyses have shown that the accuracy drop can additionally be attributed to (i) Using ReLU as the default choice for activation functions unanimously, and (ii) Fine-tuning SNNs with the same hyperparameters as dense counterparts. Thus, we focus on learning a novel way to tune activation functions for sparse networks and combining these with a separate hyperparameter optimization (HPO) regime for sparse networks. By conducting experiments on popular DNN models (LeNet-5, VGG-16, ResNet-18, and EfficientNet-B0) trained on MNIST, CIFAR-10, and ImageNet-16 datasets, we show that the novel combination of these two approaches, dubbed Sparse Activation Function Search, short: SAFS, results in up to 15.53%, 8.88%, and 6.33% absolute improvement in the accuracy for LeNet-5, VGG-16, and ResNet-18 over the default training protocols, especially at high pruning ratios.[1]

1 Introduction

Deep Neural Networks, while having demonstrated strong performance on a variety of tasks, are computationally expensive to train and deploy. When combined with concerns about privacy, energy efficiency, and the lack of stable connectivity, this led to an increased interest in deploying DNNs on resource-constrained devices like micro-controllers and FPGAs (Chen and Ran, 2019).

Recent works have tried to address this problem by reducing the enormous memory footprint and power consumption of DNNs. These include quantization (Zhou et al., 2017), knowledge distillation (Hinton et al., 2015), low-rank decomposition (Jaderberg et al., 2014), and network sparsification using unstructured pruning (a.k.a. Sparse Neural Networks) (Han et al., 2015). Among these, Sparse Neural Networks (SNNs) have shown considerable benefit through their ability to remove redundant weights (Hoefler et al., 2021). However, they suffer from accuracy drop, especially at high pruning ratios; e.g., Mousavi et al. (2022) report ≈54% reduction in top-1 accuracy for MobileNet-v2 (Sandler et al., 2018) trained on ImageNet as compared to non-pruned. While significant blame for this accuracy drop goes to sparsification itself, we identified two underexplored, pertinent factors that can additionally impact it: (i) The activation functions of the sparse counterparts are never optimized, with the Rectified Linear Unit (ReLU) (Nair and Hinton, 2010) being the default choice. (ii) The training hyperparameters of the sparse neural networks are usually kept the same as their dense counterparts.

A natural step, thus, is to understand how the activation functions impact the learning process for SNNs. Previously, Jaiswal et al. (2022) and Tessera et al. (2021) have demonstrated that ReLU reduces the trainability of SNNs since sudden changes in gradients around zero result in blocking gradient flow. Additionally, Apicella et al. (2021) have shown that a ubiquitous activation function cannot prevent typical learning problems such as vanishing gradients. While the field of Automated

[1]Our code is available at anon-github.automl.cc/r/SAFS-B67D

Machine Learning (AutoML) (Hutter et al., 2019) has previously explored optimizing activation functions of dense DNNs (Ramachandran et al., 2018; Loni et al., 2020; Bingham et al., 2020), most of these approaches require a huge amount of computing resources (up to 2000 GPU hours (Bingham et al., 2020)), resulting in a lack of interest in activation function optimization for various deep learning problems. On the other hand, attempts to improve the accuracy of SNNs either use sparse architecture search (Fedorov et al., 2019; Mousavi et al., 2022) or sparse training regimes (Srinivas et al., 2017). To our knowledge, there is no efficient approach for optimizing activation functions on SNN training.

Paper Contributions: (i) We analyze the impact of activation functions and training hyperparameters on the performance of sparse CNN architectures. (ii) We propose a novel AutoML approach, dubbed SAFS, to tweak the activation functions and training hyperparameters of sparse neural networks to deviate from the training protocols of their dense counterparts. (iii) We demonstrate significant performance gains when applying SAFS with unstructured magnitude pruning to LeNet-5 on the MNIST (LeCun et al., 1998) dataset, VGG-16 and ResNet-18 networks trained on the CIFAR-10 (Krizhevsky et al., 2014) dataset, and ResNet-18 and EfficientNet-B0 networks trained on the ImageNet-16 (Chrabaszcz et al., 2017) dataset, when compared against the default training protocols, especially at high levels of sparsity.

2 Related Work

To the best of our knowledge, SAFS is the first automated framework that tweaks the activation functions of sparse neural networks using a multi-stage optimization method. Our study also sheds light on the fact that tweaking the hyperparameters plays a crucial role in the accuracy of sparse neural networks. Improving the accuracy of sparse neural networks has been extensively researched in the past. Prior studies are mainly categorized as (i) recommending various criteria for selecting insignificant weights, (ii) pruning at initialization or training, and (iii) optimizing other aspects of sparse networks apart from pruning criteria. In this section, we discuss these methods and compare them with SAFS, and briefly review state-of-the-art research on optimizing activation functions of dense networks.

2.1 Sparse Neural Network Optimization

Pruning Insignificant Weights. A number of studies have proposed to prune the weight parameters below a fixed threshold, regardless of the training objective (Han et al., 2015; Li et al., 2016; Zhou et al., 2019). Recently, Azarian et al. (2020) and Kusupati et al. (2020) suggested layer-wise trainable thresholds for determining the optimal value for each layer.

Pruning at Initialization or Training. These methods aim to start sparse instead of first pre-training a dense network and then pruning it. To determine which weights should remain active at initialization, they use criteria such as using the connection sensitivity (Lee et al., 2018) and conservation of synaptic saliency (Tanaka et al., 2020). On the other hand, Mostafa and Wang (2019); Mocanu et al. (2018); Evci et al. (2020) proposed to leverage information gathered during the training process to dynamically update the sparsity pattern of kernels.

Miscellaneous Sparse Network Optimization. Evci et al. (2019) investigated the loss landscape of sparse neural networks and Frankle et al. (2020) addressed how it is impacted by the noise of Stochastic Gradient Descent (SGD). Finally, Lee et al. (2020) studied the effect of weight initialization on the performance of sparse networks. While our work also aims to improve the performance of sparse networks and enable them to achieve the same performance as their dense counterparts, we instead focus on the impact of optimizing activation functions and hyperparameters of the sparse neural networks in a joint HPO setting.

2.2 Activation Function Search

Inappropriate selection of activation functions results in information loss during forward propagation and the vanishing and/or exploding gradient problems during backpropagation (Hayou et al., 2019). To find the optimal activation functions, several studies automatically tuned activation functions for dense DNNs, being based on either evolutionary computation (Bingham et al., 2020; Basirat and Roth, 2021; Nazari et al., 2019), reinforcement learning (Ramachandran et al., 2018), or gradient descent for devising parametric functions (Tavakoli et al., 2021; Zamora et al., 2022).

Despite the success of these methods, automated tuning of activation functions for dense networks is unreliable for the sparse context since the search spaces for activation functions for dense networks are not optimal for sparse networks (Dubowski, 2020). The same operations that are successful in dense networks can drastically diminish network gradient flow in sparse networks (Tessera et al., 2021). Additionally, existing methods suffer from significant search costs; e.g., Bingham et al. (2020) required 1000 GPU hours per run on NVIDIA® GTX 1080Ti. Jin et al. (2016) showed the superiority of SReLU over ReLU when training sparse networks as it improves the network's gradient flow. However, SReLU requires learning four additional parameters per neuron. In the case of deploying networks with millions of hidden units, this can easily lead to considerable computational and memory overhead at inference time. `SAFS`, on the other hand, unifies local search on a meta-level with gradient descent to create a two-tier optimization strategy and obtains superior performance with faster search convergence compared to the state-of-the-art.

3 Preliminaries

In this section, we develop notations for the later sections by formally introducing the two problems that we address: Network Sparsification and Hyperparameter Optimization.

3.1 Network Sparsification

Network sparsification is an effective technique to improve the efficiency of DNNs for applications with limited computational resources. Zhan and Cao (2019) reported that network sparsification could facilitate saving ResNet-18 inference time trained on ImageNet on mobile devices by up to 29.5×. Network sparsification generally consists of three stages:

1. *Pre-training*: Train a large, over-parameterized model. Given a loss metric $\mathcal{L}_{train}$ and network parameters $\boldsymbol{\theta}$, this can be formulated as the task of finding the parameters $\boldsymbol{\theta}^{\star}_{pre}$ that minimize $\mathcal{L}_{train}$ on training data $\mathcal{D}_{train}$:

$$\boldsymbol{\theta}^{\star}_{pre} \in \underset{\boldsymbol{\theta}\in\boldsymbol{\Theta}}{\operatorname{argmin}} \left[\mathcal{L}_{train}(\boldsymbol{\theta}; \mathcal{D}_{train})\right] \tag{1}$$

2. *Pruning*: Having trained the dense model, the next step is to remove the low-importance weight tensors of the pre-trained network. This can be done layer-wise, channel-wise, and network-wide. The usual mechanisms either simply set a certain percentage of weights (*pruning ratio*) to zero, or learn a Boolean mask $\boldsymbol{m}^{\star}$ over the weight vector. Both of these notions can be generally captured in a manner similar to the dense training formulation but with a separate loss metric $\mathcal{L}_{prune}$. The objective here is to obtain a pruning mask $\boldsymbol{m}^{\star}$, where $\odot$ represents the masking operation and N represents the size of the mask:

$$\boldsymbol{m}^{\star} \in \underset{\boldsymbol{m}\in\{0,1\}^{N}}{\operatorname{argmin}} \left[\mathcal{L}_{prune}(\boldsymbol{\theta}^{\star}_{pre} \odot \boldsymbol{m}; \mathcal{D}_{train})\right] \quad \text{s.t.} \quad \|\boldsymbol{m}^{\star}\|_0 \leq \epsilon \tag{2}$$

where ϵ is a threshold on the minimal number of masked weights.

3. *Fine-tuning*: The final step is to retrain the pruned network to regain its original accuracy using a fine-tuning [2] loss $\mathcal{L}_{fine}$, which can either be the same as the training loss, or a different kind:

$$\boldsymbol{\theta}^{\star}_{fine} \in \underset{\boldsymbol{\theta} \in \boldsymbol{\Theta}}{\operatorname{argmin}} \left[\mathcal{L}_{fine}(\boldsymbol{\theta}; \boldsymbol{\theta}^{\star}_{pre} \odot \boldsymbol{m}^{\star}, \mathcal{D}_{train}) \right] \tag{3}$$

For the pruning stage, SAFS uses the popular magnitude pruning method (Han et al., 2015) by removing a certain percentage of weights that have a lower magnitude. Compared to structured pruning methods (Liu et al., 2018), the magnitude pruning method provides higher flexibility and a better compression rate $\left(\frac{|\boldsymbol{\theta}^{\star}_{fine}|}{|\boldsymbol{\theta}^{\star}_{pre}|} \times 100 \right)$. Crucially, SAFS is independent of the pruning algorithm; thus, it can optimize any sparse network.

3.2 Hyperparameter Optimization (HPO)

We denote the hyperparameter space of the model as Λ out of which we sample a hyperparameter configuration $\boldsymbol{\lambda} = (\lambda_1, \ldots, \lambda_d)$ to be tuned by some HPO methods. We assume $c : \boldsymbol{\lambda} \rightarrow \mathbb{R}$ to be a black-box cost function that maps the selected configuration $\boldsymbol{\lambda}$ to a performance metric, such as model-error[3]. HPO's goal can then be summarized as the task of finding an optimal configuration $\boldsymbol{\lambda}^{\star}$ minimizing c. Given the fine-tuned parameters $\boldsymbol{\theta}^{\star}_{fine}$ obtained in Equation (3), we define the cost as minimizing a loss $\mathcal{L}_{hp}$ on validation dataset $\mathcal{D}_{val}$ as a bi-level optimization problem:

$$\begin{aligned} \boldsymbol{\lambda}^{\star} \in \underset{\boldsymbol{\lambda} \in \Lambda}{\operatorname{argmin}}\, c(\boldsymbol{\lambda}) &= \underset{\boldsymbol{\lambda} \in \Lambda}{\operatorname{argmin}} \left[\mathcal{L}_{hp}(\boldsymbol{\theta}^{\star}_{fine}(\boldsymbol{\lambda}); \mathcal{D}_{val}) \right] \\ &\text{s.t.} \\ \boldsymbol{\theta}^{\star}_{fine}(\boldsymbol{\lambda}) \in \underset{\boldsymbol{\theta} \in \boldsymbol{\Theta}}{\operatorname{argmin}} &\left[\mathcal{L}_{fine}(\boldsymbol{\theta}; \boldsymbol{\theta}^{\star}_{pre} \odot \boldsymbol{m}^{\star}, \mathcal{D}_{train}, \boldsymbol{\lambda}) \right] \end{aligned} \tag{4}$$

We note that in principle HPO could also be applied to the training of the original model (Equation (1)), but we assume that the original is given and we care only about sparsification.

4 Finding Activation Functions for Sparse Networks

The aim of SAFS is to find an optimal hyperparameter configuration for pruned networks with a focus on activation functions. Given the HPO setup described in Section 3.2, we now explain how to formulate the activation function search problem and what is needed to solve it.

4.1 Modelling Activation Functions

Using optimization techniques requires creating a search space containing promising candidate activation functions. Extremely constrained search spaces might not contain novel activation functions (*expressivity*) while searching in excessively large search spaces can be difficult (*size*) (Ramachandran et al., 2018). Thus, striking a balance between the expressivity and size of the search space is an important challenge in designing search spaces.

To tackle this issue, we model parametric activation functions as a combination of a unary operator f and two learnable scaling factors α, β. Thus, given an input x and output y, the activation function can be formulated as $y = \alpha f(\beta x)$, which can alternatively be represented as a computation graph shown in Figure 3a.

Figure 1 illustrates an example of tweaking the α and β learnable parameters of the *Swish* activation function. We can intuitively see that modifying the suggested learnable parameters for a

[2] We use the term fine-tuning interchangeably with re-training

[3] For reasonably sized datasets and models, we estimate this error using k-fold cross-validation.

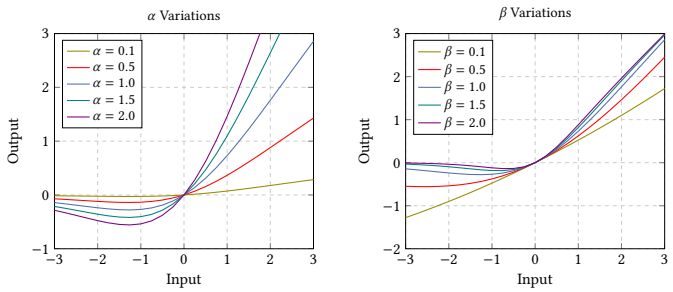

(a) **(b)**

Figure 1: Modifying (a) α and (b) β learnable scaling factors of the *Swish* activation function.

sample unary operator provides the sparse network additional flexibility to fine-tune activation functions (Godfrey, 2019; Bingham and Miikkulainen, 2022). Examples of activation functions that we consider in this work have been listed in Appendix E.

For sparse networks, this representation allows efficient implementation as well as effective parameterization. As we explain further in Section 4.2, by treating this as a two-stage optimization process, where the search for f is a discrete optimization problem and the search for α, β is interleaved with fine-tuning, we are able to make the search process efficient while capturing the essence of input-output scaling and functional transformations prevalent with activation functions. Note that SAFS falls under the category of adaptive activation functions due to introducing trainable parameters (Dubey et al., 2022). These parameters allow the activation functions to smoothly adjust the model with the dataset complexity (Zamora et al., 2022). In contrast to popular adaptive activation functions such as PReLU and Swish, SAFS automates activation function tuning across a diverse family of activation functions for each layer of the network with optimized hyperparameters.

4.2 Optimization Procedure

SAFS performs the optimization layer-wise i.e. we intend to find the activation functions for each layer. Given layer indices $i = 1, \ldots, L$ of the network of depth L an optimization algorithm needs to be able to select a unary operator $f_i^\star$ and find appropriate scaling factors $(\alpha_i^\star, \beta_i^\star)$. We formulate these as two independent objective functions, solved in a two-stage optimization procedure combining discrete and stochastic optimization. Figure 2 shows an overview of the SAFS pipeline.

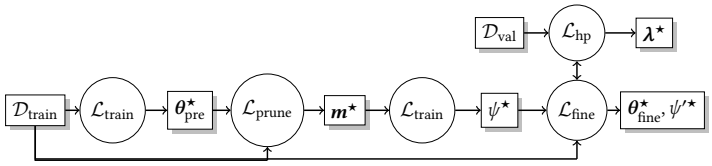

Figure 2: Overview of the entire SAFS pipeline.

Stage 1: Unary Operator Search. The first stage is to find the unary operators after the network has been pruned. Crucially, the fine-tuning step happens only after this optimization for the activation function has been completed. We model the task of finding optimal unary operators for each layer as a discrete optimization problem. Given a pre-defined set of functions $F = \{f_1, f_2, \ldots, f_n\}$, we define a space $\mathcal{F}$ of possible sequences of operators $\psi = \langle f_i \mid f_i \in F \rangle_{i \in \{1,\ldots,L\}} \in \mathcal{F}$ of size L. Our task is to find a sequence ψ after the pruning stage (Item 2). Since the pre-trained network parameters $\boldsymbol{\theta}^\star_{pre}$ and the pruning mask $\boldsymbol{m}^\star$ have already been discovered, we keep them fixed and use them as an initialization point for activation function optimization. The task is formulated as finding the

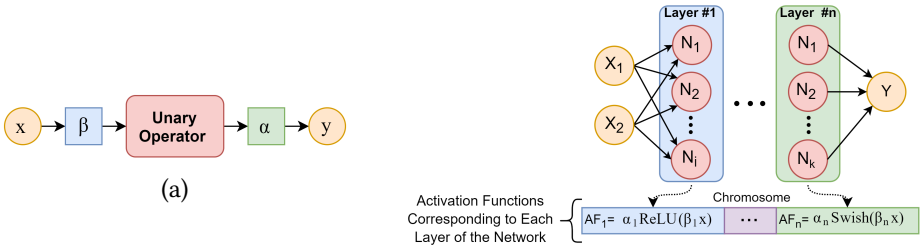

(a) (b)

Figure 3: (a) SAFS unary activation graph. (b) An example of a solution representing activation functions of each layer in the network.

optimal operators given the network parameters, as shown in Equation (5). During this step, α and β parameters are set to 1 to focus on the function class first.

$$\psi^\star \in \underset{\psi \in \mathcal{F}}{\operatorname{argmin}} \left[\mathcal{L}_{train}(\boldsymbol{\theta}^\star_{pre} \odot \boldsymbol{m}^\star, \psi; \mathcal{D}_{train}) \right] \tag{5}$$

Given the discrete nature of Equation (5), we use Late Acceptance Hill Climbing (LAHC) (Burke and Bykov, 2017) to iteratively solve it (Please refer to Appendix A for comparison against other search algorithms). LAHC is a Hill Climbing algorithm that uses a record of the history - *History Length* - of objective values of previously encountered solutions in order to decide whether to accept a new solution. It provides us with two benefits: (i) Being a semi-local search method, LAHC works on discrete spaces and quickly searches the space to find unary operators. (ii) LAHC extends the vanilla hill-climbing algorithm (Selman and Gomes, 2006) by allowing worse solutions in the hope of finding a better solution in the future. We represent the design space of LAHC using a chromosome that is a list of activation functions corresponding to each layer of the network. Figure 3b shows an example of a solution in the design space. The benefit of this representation is its flexibility and simplicity. For generating a new search candidate (*mutation operation*), we first swap two randomly selected genes from the chromosome, and then, we randomly changed one gene from the chromosome with a new candidate from the list.

Appendix E lists unary operators considered in this study. To avoid instability during training, we ignored periodic operators (e.g., $cos(x)$) and operators containing horizontal ($y = 0$) or vertical ($x = 0$) asymptotes (e.g., $y = \frac{1}{x}$).

The process of selecting operators to form the chromosome is repeated for a predefined number of iterations (refer to Appendix E for the configuration of LAHC). Given that we have only two mutations per each search iteration, the entire chromosome is not significantly affected. Based on trial runs, we determined a budget of 20 search iterations to provide decent improvement alongside reducing the search cost. Each iteration consists of training the network using the selection activation functions and measuring the training loss $\mathcal{L}_{train}$ as a fitness metric that needs to be minimized.

A downside of this process is the need to retrain the network for each search iteration, which can be intensive in time and compute resources. We circumvent this issue by leveraging a lower fidelity estimation of the final performance. Given that the network performance does not vary after a certain number of epochs, we leverage the work by Loni et al. (2020) and only train the network up to a certain point after which the performance should remain stable.

Stage 2: Scaling Factor and HPO Given a learned sequence of optimal operators ψ, the next step is to find a sequence $\psi' = \langle (\alpha_i, \beta_i) \mid \alpha_i, \beta_i \in \mathbb{R} \rangle_{i \in \{1,\dots,L\}}$ representing the scaling factors for each layer. We perform this process jointly with the fine-tuning stage (Equation (3)) and HPO to discover the fine-tuning parameters $\boldsymbol{\theta}^\star_{fine}$ and hyperparameters $\boldsymbol{\lambda}^\star$ as shown in Equation (6).

$$\boldsymbol{\lambda}^{\star} \in \underset{\boldsymbol{\lambda}\in\Lambda}{\operatorname{argmin}}\, c(\boldsymbol{\lambda}; \mathcal{D}_{val}) \quad \text{s.t.} \quad \psi'^{\star}, \boldsymbol{\theta}^{\star}_{fine}(\boldsymbol{\lambda}) \in \underset{\theta\in\boldsymbol{\Theta},\psi'\in\mathcal{R}^{(2,L)}}{\operatorname{argmin}} \left[\mathcal{L}_{fine}\big((\boldsymbol{\theta} \mid \boldsymbol{\theta}^{\star}_{pre} \odot \boldsymbol{m}^{\star}), \psi'; \psi, \mathcal{D}_{train}\big)\right] \tag{6}$$

Due to the continuous nature of this stage, we use the Stochastic Gradient Descent (SGD) for solving Equation (6), and use the validation accuracy as a fitness metric for the hyperparameter configuration.

Treating the scaling factors as learnable parameters allows us to learn them during the fine-tuning state. Thus, the inner optimization in this step has nearly no overhead costs. The only additional cost is that of HPO, which we demonstrate in our experiments to be important and worth it since the hyperparameters from training the original model might not be optimal for fine-tuning.

5 Experiments

We categorize the experiments based on the research questions this work aims to answer. Section 5.1 introduces the experimental setup. Section 5.2 motives the problem of tuning activation functions for SNNs. Section 5.3 introduces the need for HPO with activation tuning for SNNs. In Section 5.4, we compare SAFS against different baselines. Appendix C provides an accuracy improvement vs. compression ratio trade-off to compare SAFS with state-of-the-art network compression methods. In Section 5.5 we compare the performance of SAFS for various pruning ratios. In Section 5.6 we provide insights on the activation functions learned by SAFS. Finally, we ablate SAFS in Section 5.7 to determine the impact of different design choices.

5.1 Experimental Setup

Datasets. To evaluate SAFS, we use MNIST (LeCun et al., 1998), CIFAR-10 (Krizhevsky et al., 2014) and ImageNet-16 (Chrabaszcz et al., 2017) public classification datasets. Note that ImageNet-16 includes all images of the original ImageNet dataset, resized to 16×16 pixels. All HPO experiments were conducted using SMAC3 (Lindauer et al., 2022). Appendix E presents the rest of the experimental setup.

5.2 The Impact of Tweaking Activation Functions on the Accuracy of SNNs

To validate the assumption that activation functions indeed impact the accuracy, we investigated whether activation functions currently used for dense networks (Evci et al., 2022) are still reliable in the sparse context. Figure 4a shows the impact of five different activation functions on the accuracy of sparse architectures with various pruning ratios. To measure the performance during the search stage, we use a three-fold validation approach. However, we report the test accuracy of SAFS to compare our results with other baselines.

Our conclusions from this experiment can be summarised as follows: (i) ReLU does not perform the best in all scenarios. We see that SRS, Swish, Tanh, Symlog, FLAU, and PReLU outperform ReLU on higher sparsity levels. Thus, the decision to use ReLU unanimously can limit the potential gain in accuracy. (ii) As we increase the pruning ratio to 99% (extremely sparse networks), despite the general drop in accuracy, the difference in the sparse and dense networks' accuracies vary greatly depending on the activation function. Thus, the choice of activation function for highly sparse networks becomes an important parameter. We need to mention that despite the success of SAFS in providing higher accuracy, it needs 47 GPU hours in total for learning activation functions and optimal HPs. On the other hand, refining a sparse neural network takes ≈ 3.9 GPU hours.

5.3 The Difficulty of Training Sparse Neural Networks

Currently, most algorithms for training sparse DNNs use configurations customized for their dense counterparts, e.g., starting from a fixed learning scheduler. To validate the need for optimizing the

training hyperparameters of the sparse networks, we used the dense configurations as a baseline against hyperparameters learned by an HPO method. Figure 4b shows the curves of fine-tuning sparsified VGG-16 with 99% pruning ratio trained on CIFAR-10. The training has been performed with the hyperparameters of the dense network (Blue), and training hyperparameters optimized using SMAC3 (Orange).

We optimized the learning rate, learning rate scheduler, and optimizer hyperparameters with the range specified in Appendix E (Table 4). The type and range of hyperparameters are selected based on recommended ranges from deep learning literature (Simonyan and Zisserman, 2014; Subramanian et al., 2022; Zimmer et al., 2021), SMAC3 documentation (Lindauer et al., 2022), and from the various open-source libraries[4] used to implement VGG-16. To prevent overfitting on the test data, we optimized the hyperparameters on validation data and tested the final performance on the test data. The poor performance (7.17% accuracy reduction) of the SNN learning strategy using dense parameters motivates the need for a separate sparsity-aware HPO regime.

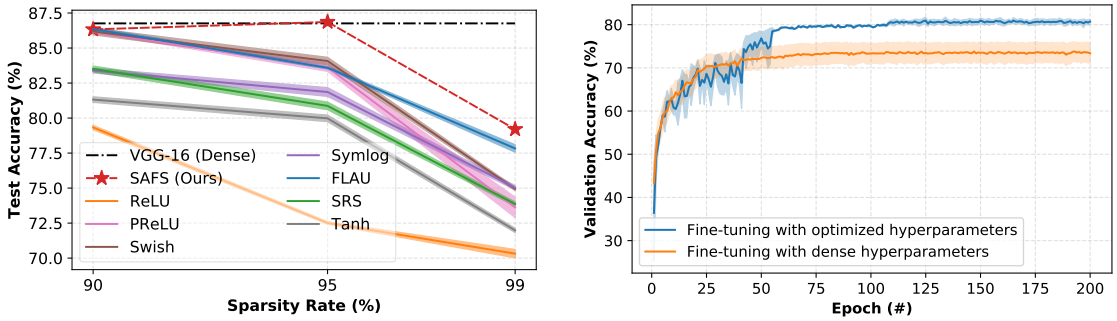

(a) (b)

Figure 4: (a) CIFAR-10 test accuracy on sparse VGG-16 with various activation functions customized for dense networks with a 3-fold cross-validation procedure. The bold line represents the mean across the folds, while the shaded area represents the Confidence Intervals across the folds. (b) Fine-tuning sparse VGG-16 on CIFAR-10 with different training hyperparameters with three different random seeds. The pruning ratio is 99%. As shown, fine-tuning with dense hyperparameters results in inefficient training of SNNs.

5.4 Comparison with Magnitude Pruning Baselines

Table 1 shows the results of optimizing sparse VGG-16 activation functions trained on CIFAR-10 using SAFS with 99% pruning ratio. An average of three runs has been reported. Results show that SAFS provides 8.88% absolute accuracy improvement for VGG-16 and 6.33% for ResNet-18 trained on CIFAR-10 when compared against a vanilla magnitude pruning baseline. SAFS additionally yields 1.8% absolute Top-1 accuracy improvement for ResNet-18 and 1.54% for EfficientNet-B0 trained on ImageNet-16 when compared against a vanilla magnitude pruning baseline. SReLU (Jin et al., 2016) is a piece-wise linear activation function that is formulated by four learnable parameters. Mocanu et al. (2018); Curci et al. (2021); Tessera et al. (2021) have shown SReLU performs excellently for sparse neural networks due to improving the network's gradient flow. Results show that SAFS provides 15.99% and 19.17% higher accuracy compared to training VGG-16 and ResNet-18 with SReLU activation function on CIFAR-10. Plus, SAFS provides 0.88% and 1.28% better accuracy compared to training ResNet-18 and EfficientNet-B0 with SReLU activation function on the ImageNet-16 dataset.

[4] https://www.kaggle.com/datasets/keras/vgg16/code

Table 1: Refining sparse neural network activation functions with different methods.

Magnitude Pruning (Han et al., 2015)	CIFAR-10 (Top-1)		ImageNet-16‡ (Top-1 / Top-5)	
	VGG-16	ResNet-18	ResNet-18	EfficientNet-B0
Original Model (Dense)	86.76%	89.86%	25.42% / 47.26%	18.41% / 37.45%
Vanilla Pruning (Baseline)	70.32%	77.55%	11.32% / 25.59%	10.96% / 25.62%
SReLU	63.21%	64.71%	12.24% / 26.89%	11.22% / 25.98%
SAFS (Ours)	79.2% (+8.88%)	83.88% (+6.33%)	13.12% (+1.8%) / 28.94%	12.5% (+1.54%) / 27.15%

‡ The Top-1 accuracy of WideResNet-20-1 on ImageNet-16 is 14.82% (Chrabaszcz et al., 2017).

5.5 Evaluation of SAFS with Various Pruning Ratios

Figure 4a compares the performance of VGG-16 fine-tuned by SAFS and the default training protocol on CIFAR-10 over three different pruning ratios including 90%, 95%, and 99%. Results show that SAFS is extremely effective by achieving 1.65%, 7.45%, and 8.88% higher accuracies compared to VGG-16 with ReLU activation functions fine-tuned with the default training protocol at 90%, 95%, and 99% pruning ratios. Plus, SAFS is better than activation functions designed for dense networks, especially for networks with a 99% pruning ratio.

5.6 Insights on Searching for Activation Functions

Figure 5 presents the dominance pattern of each unary operator in the first learning stage ($\alpha = \beta = 1$) for the CIFAR-10 dataset. The results are the average of three runs with different random seeds. The unit of the color bar is the number of seeing a specific activation function across all search iterations for the first learning stage. According to the results, it is evident that (i) Symexp and ELU are unfavorable activation functions, (ii) Symlog and Acon are dominant activation functions while being used in the early layers, and (iii) Overall Swish and HardSwish are good, but they mostly appear in the middle layers.

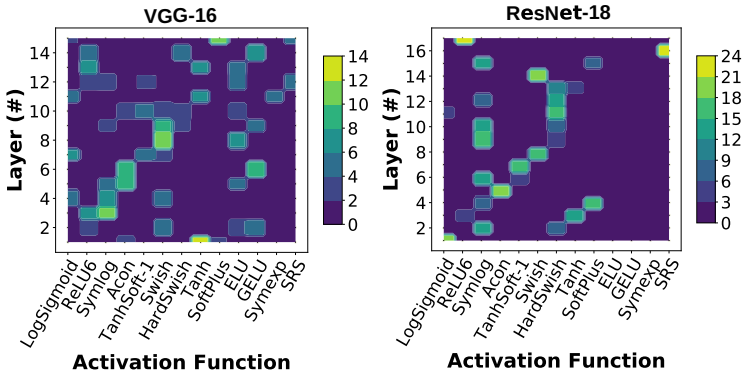

Figure 5: Frequency of Occurring unary operator in the first learning stage ($\alpha = \beta = 1$) for VGG-16 and ResNet-18 trained on CIFAR-10 with 99% pruning ratio.

5.7 Ablation Study

We study the effect of each individual optimization stage of SAFS on the performance of sparse VGG-16 and ResNet-18 trained on CIFAR-10 in Table 2. Results show that each individual contribution provides higher accuracy for both VGG-16 and ResNet-18. However, the maximum performance is attained by SAFS (+15.53%, +8.88%, +6.33%, and +1.54% for LeNet-5, VGG-16, ResNet-18, and EfficientNet-B0), where we first learn the most accurate unary operator for each layer and then fine-tune scaling factors with optimized hyperparameters.

Table 2: Ablation Study on optimizing activation functions of SNNs with 99% pruning ratio.

CNN Model⋆	Dense Model	Magnitude Pruning	Learning Activation Functions∓		
			(Stage 1)†	(Stage 2)‡	SAFS (Stage 1 + Stage 2)
LeNet-5	98.49%	46.69%	61.63%	60.2%	62.22% (+15.53%)
VGG-16	86.76%	70.32%	78.11%	80.97%	79.2% (+8.88%)
ResNet-18	89.86%	77.55%	79.34%	82.74%	83.88% (+6.33%)
EfficientNet-B0	18.41%	10.96%	11.84%	11.7%	12.5% (+1.54%)

⋆ Lenet-5, VGG-16, ResNet-18, and EfficientNet-B0 are trained on MNIST, CIFAR-10, CIFAR-10, and ImageNet-16, respectively.
∓ ReLU is the default activation function for Lenet-5, VGG-16, and ResNet-18. Swish is the default activation function for EfficientNet-B0.
† Learning activation functions by only using the first stage of SAFS ($\alpha = \beta = 1$ and without using HPO).
‡ Learning α and β for the ReLU operator with optimized hyperparameters.

6 Conclusion

In this paper, we studied the impact of activation functions on training sparse neural networks and use this to learn new activation functions. To this end, we demonstrated that the accuracy drop incurred by training SNNs uniformly with ReLU for all units can be partially mitigated by a layer-wise search for activation functions. We proposed a novel two-stage optimization pipeline that combines discrete and stochastic optimization to select a sequence of activation functions for each layer of an SNN, along with discovering the optimal hyperparameters for fine-tuning. Our method SAFS provides significant improvement by achieving up to 8.88% and 6.33% higher accuracy for VGG-16 and ResNet-18 on CIFAR-10 over the default training protocols, especially at high pruning ratios. Crucially, since SAFS is independent of the pruning algorithm, it can optimize any sparse network.

7 Limitations and Broader Impact

Limitations. The authors have determined that this work will have no negative impacts on society or the environment.

Broader Impact and Future Work. Sparse Neural Networks (SNNs) enable the deployment of large models on resource-limited devices by saving computational costs and memory consumption. In addition, this becomes important in view of decreasing the carbon footprint and resource usage of DNNs at inference time. We believe this opens up new avenues of research into methods that can improve the accuracy of SNNs. We hope that our work motivates engineers to use SNNs more than before in real-world products as SAFS provides SNNs with similar performance to dense counterparts. Some immediate directions for extending our work are (i) leveraging the idea of accuracy predictors (Li et al., 2023) in order to expedite the search procedure. (ii) SNNs have recently shown promise in application to techniques for sequential decision-making problems such as Reinforcement Learning (Vischer et al., 2022; Graesser et al., 2022). We believe incorporating SAFS into such scenarios can help with the deployability of such pipelines.

SAFS has been evaluated on diverse datasets, including MNIST, CIFAR-10, and ImageNet-16, and various network architectures such as LeNet-5, VGG-16, ResNet-18, and EfficientNet-B0. While the current results demonstrate the general applicability of our method and signs of scalability, we believe further experiments on larger datasets and more scalable networks would be an interesting avenue for future work.

8 Reproducibility Checklist

1. For all authors...

   (a) Do the main claims made in the abstract and introduction accurately reflect the paper's contributions and scope? [Yes]

   (b) Did you describe the limitations of your work? [Yes]

(c) Did you discuss any potential negative societal impacts of your work? [Yes]

(d) Have you read the ethics author's and review guidelines and ensured that your paper conforms to them? https://automl.cc/ethics-accessibility/ [Yes]

2. If you are including theoretical results...

(a) Did you state the full set of assumptions of all theoretical results? [N/A]

(b) Did you include complete proofs of all theoretical results? [N/A]

3. If you ran experiments...

(a) Did you include the code, data, and instructions needed to reproduce the main experimental results, including all requirements (e.g., `requirements.txt` with explicit version), an instructive README with installation, and execution commands (either in the supplemental material or as a URL)? [Yes]

(b) Did you include the raw results of running the given instructions on the given code and data? [Yes]

(c) Did you include scripts and commands that can be used to generate the figures and tables in your paper based on the raw results of the code, data, and instructions given? [Yes]

(d) Did you ensure sufficient code quality such that your code can be safely executed and the code is properly documented? [Yes]

(e) Did you specify all the training details (e.g., data splits, pre-processing, search spaces, fixed hyperparameter settings, and how they were chosen)? [Yes]

(f) Did you ensure that you compared different methods (including your own) exactly on the same benchmarks, including the same datasets, search space, code for training and hyperparameters for that code? [Yes] Appendix A compares different search methods for solving Equation (5).

(g) Did you run ablation studies to assess the impact of different components of your approach? [Yes] Table 2

(h) Did you use the same evaluation protocol for the methods being compared? [Yes]

(i) Did you compare performance over time? [N/A]

(j) Did you perform multiple runs of your experiments and report random seeds? [Yes]

(k) Did you report error bars (e.g., with respect to the random seed after running experiments multiple times)? [Yes]

(l) Did you use tabular or surrogate benchmarks for in-depth evaluations? [No]

(m) Did you include the total amount of computing and the type of resources used (e.g., type of GPUs, internal cluster, or cloud provider)? [Yes] Table 8 lists the type of resources used in this paper. Appendix D reports the amount of compute time for the activation function optimization.

(n) Did you report how you tuned hyperparameters, and what time and resources this required (if they were not automatically tuned by your AutoML method, e.g. in a NAS approach; and also hyperparameters of your own method)? [Yes]

4. If you are using existing assets (e.g., code, data, models) or curating/releasing new assets...

(a) If your work uses existing assets, did you cite the creators? [Yes]

(b) Did you mention the license of the assets? [Yes]

(c) Did you include any new assets either in the supplemental material or as a URL? [N/A]

(d) Did you discuss whether and how consent was obtained from people whose data you're using/curating? [N/A]

(e) Did you discuss whether the data you are using/curating contains personally identifiable information or offensive content? [N/A]

5. If you used crowdsourcing or conducted research with human subjects...

(a) Did you include the full text of instructions given to participants and screenshots, if applicable? [N/A]

(b) Did you describe any potential participant risks, with links to Institutional Review Board (IRB) approvals, if applicable? [N/A]

(c) Did you include the estimated hourly wage paid to participants and the total amount spent on participant compensation? [N/A]

References

(2017). *Proceedings of the International Conference on Learning Representations (ICLR'17)*. Published online: iclr.cc.

Apicella, A., Donnarumma, F., Isgrò, F., and Prevete, R. (2021). A survey on modern trainable activation functions. *Neural Networks*, 138.

Azarian, K., Bhalgat, Y., Lee, J., and Blankevoort, T. (2020). Learned threshold pruning. *CoRR*.

Basirat, M. and Roth, P. (2021). S* relu: Learning piecewise linear activation functions via particle swarm optimization. In *Proceedings of the 16th International Joint Conference on Computer Vision, Imaging and Computer Graphics Theory and Applications*.

Bingham, G., Macke, W., and Miikkulainen, R. (2020). Evolutionary optimization of deep learning activation functions. In Ceberio, J., editor, *Proceedings of the Genetic and Evolutionary Computation Conference (GECCO'20)*.

Bingham, G. and Miikkulainen, R. (2022). Discovering parametric activation functions. *Neural Networks*.

Biswas, K., Kumar, S., Banerjee, S., and Pandey, A. K. (2021). Tanhsoft—dynamic trainable activation functions for faster learning and better performance. *IEEE Access*, 9.

Burke, E. and Bykov, Y. (2017). The late acceptance hill-climbing heuristic. *European Journal of Operational Research*.

Chaudhuri, K., Jegelka, S., Song, L., Szepesvári, C., Niu, G., and Sabato, S., editors (2022). *Proceedings of the 39th International Conference on Machine Learning (ICML'22)*, volume 162 of *Proceedings of Machine Learning Research*. PMLR.

Chaudhuri, K. and Salakhutdinov, R., editors (2019). *Proceedings of the 36th International Conference on Machine Learning (ICML'19)*, volume 97. Proceedings of Machine Learning Research.

Chen, J. and Ran, X. (2019). Deep learning with edge computing: A review. In *Proc. of the IEEE*.

Chrabaszcz, P., Loshchilov, I., and Hutter, F. (2017). A downsampled variant of ImageNet as an alternative to the CIFAR datasets. *arXiv:1707.08819 [cs.CV]*.

Curci, S., Mocanu, D., and Pechenizkiyi, M. (2021). Truly sparse neural networks at scale. *CoRR*.

Dubey, S. R., Singh, S. K., and Chaudhuri, B. B. (2022). Activation functions in deep learning: A comprehensive survey and benchmark. *Neurocomputing*, 503.

Dubowski, A. (2020). Activation function impact on sparse neural networks. *CoRR*.

Evci, U., Gale, T., Menick, J., Castro, P., and Elsen, E. (2020). Rigging the lottery: Making all tickets winners. In III and Singh (2020).

Evci, U., Ioannou, Y., Keskin, C., and Dauphin, Y. (2022). Gradient flow in sparse neural networks and how lottery tickets win. In Sycara et al. (2022).

Evci, U., Pedregosa, F., Gomez, A., and Elsen, E. (2019). The difficulty of training sparse neural networks. *CoRR*.

Fedorov, I., Adams, R., Mattina, M., and Whatmough, P. (2019). Sparse: Sparse architecture search for cnns on resource-constrained microcontrollers. In Wallach et al. (2019).

Frankle, J., Dziugaite, G., Roy, D., and Carbin, M. (2020). Linear mode connectivity and the lottery ticket hypothesis. In III and Singh (2020).

Godfrey, L. B. (2019). An evaluation of parametric activation functions for deep learning. In *IEEE International Conference on Systems, Man and Cybernetics*.

Graesser, L., Evci, U., Elsen, E., and Castro, P. (2022). The state of sparse training in deep reinforcement learning. In Chaudhuri et al. (2022).

Hafner, D., Pasukonis, J., Ba, J., and Lillicrap, T. (2023). Mastering diverse domains through world models. *CoRR*.

Han, S., Pool, J., Tran, J., and Dally, W. (2015). Learning both weights and connections for efficient neural network. In Cortes, C., Lawrence, N., Lee, D., Sugiyama, M., and Garnett, R., editors, *Proceedings of the 28th International Conference on Advances in Neural Information Processing Systems (NeurIPS'15)*.

Hayou, S., Doucet, A., and Rousseau, J. (2019). On the impact of the activation function on deep neural networks training. In Chaudhuri and Salakhutdinov (2019).

Hinton, G., Vinyals, O., and Dean, J. (2015). Distilling the knowledge in a neural network. *CoRR*.

Hoefler, T., Alistarh, D., Ben-Nun, T., D, N., and Peste, A. (2021). Sparsity in deep learning: Pruning and growth for efficient inference and training in neural networks. *Journal of Machine Learning Research*.

Howard, A. G., Zhu, M., Chen, B., Kalenichenko, D., Wang, W., Weyand, T., Andreetto, M., and Adam, H. (2017). Mobilenets: Efficient convolutional neural networks for mobile vision applications. *CoRR*.

Huang, Q., Zhou, K., You, S., and Neumann, U. (2018). Learning to prune filters in convolutional neural networks. In *2018 IEEE Winter Conference on Applications of Computer Vision (WACV)*.

Hubens, N., Mancas, M., Gosselin, B., Preda, M., and Zaharia, T. (2022). One-cycle pruning: Pruning convnets with tight training budget. In *2022 IEEE International Conference on Image Processing (ICIP)*.

Hutter, F., Kotthoff, L., and Vanschoren, J., editors (2019). *Automated Machine Learning: Methods, Systems, Challenges*. Springer. Available for free at http://automl.org/book.

III, H. D. and Singh, A., editors (2020). *Proceedings of the 37th International Conference on Machine Learning (ICML'20)*, volume 98. Proceedings of Machine Learning Research.

Ilboudo, W., Eric, L., Kobayashi, T., and Sugimoto, K. (2020). Tadam: A robust stochastic gradient optimizer. *CoRR*.

Jaderberg, M., Vedaldi, A., and Zisserman, A. (2014). Speeding up convolutional neural networks with low rank expansions. In *British Machine Vision Conference, BMVC*.

Jaiswal, A., Ma, H., Chen, T., Ding, Y., and Wang, Z. (2022). Training your sparse neural network better with any mask. In Chaudhuri et al. (2022).

Jin, X., Xu, C., Feng, J., Wei, Y., Xiong, J., and Yan, S. (2016). Deep learning with s-shaped rectified linear activation units. In Schuurmans, D. and Wellman, M., editors, *Proceedings of the Thirtieth AAAI Conference on Artificial Intelligence (AAAI'16)*. AAAI Press.

Krizhevsky, A., Nair, V., and Hinton, G. (2009). Cifar-10 and cifar-100 datasets. *URl: https://www. cs. toronto. edu/kriz/cifar. html*.

Krizhevsky, A., Nair, V., and Hinton, G. (2014). The cifar-10 dataset. *online: http://www.cs.toronto.edu/kriz/cifar.html*, 55.

Kusupati, A., Ramanujan, V., Somani, R., Wortsman, M., Jain, P., Kakade, S., and Farhadi, A. (2020). Soft threshold weight reparameterization for learnable sparsity. In III and Singh (2020).

Lacoste, A., Luccioni, A., Schmidt, V., and Dandres, T. (2019). Quantifying the carbon emissions of machine learning. *CoRR*.

Larochelle, H., Ranzato, M., Hadsell, R., Balcan, M.-F., and Lin, H., editors (2020). *Proceedings of the 33rd International Conference on Advances in Neural Information Processing Systems (NeurIPS'20)*.

LeCun, Y., Bottou, L., Bengio, Y., and Haffner, P. (1998). Gradient-based learning applied to document recognition. In *Proc. of the IEEE*.

Lee, N., Ajanthan, T., Gould, S., and Torr, P. (2020). A signal propagation perspective for pruning neural networks at initialization. In *Proceedings of the International Conference on Learning Representations (ICLR'20)*. Published online: `iclr.cc`.

Lee, N., Ajanthan, T., Lee, J., and Torr, P. H. S. (2018). Snip: Single-shot network pruning based on connection sensitivity. *CoRR*.

Li, G., Yang, Y., Bhardwaj, K., and Marculescu, R. (2023). Zico: Zero-shot nas via inverse coefficient of variation on gradients. *CoRR*.

Li, H., Kadav, A., Durdanovic, I., Samet, H., and Graf, H. P. (2016). Pruning filters for efficient convnets. *CoRR*.

Li, Y., Ding, W., Liu, C., Zhang, B., and Guo, G. (2022). Trq: Ternary neural networks with residual quantization. In Sycara et al. (2022).

Lindauer, M., Eggensperger, K., Feurer, M., Biedenkapp, A., Deng, D., Benjamins, C., Ruhkopf, T., Sass, R., and Hutter, F. (2022). SMAC3: A versatile bayesian optimization package for Hyperparameter Optimization. 23(54):1–9.

Lindauer, M. and Hutter, F. (2020). Best practices for scientific research on Neural Architecture Search. *Journal of Machine Learning Research*, 21(243):1–18.

Liu, Z., Sun, M., Zhou, T., Huang, G., and Darrell, T. (2018). Rethinking the value of network pruning. *CoRR*.

Loni, M., Mousavi, H., Riazati, M., Daneshtalab, M., and Sjödin, M. (2022). Tas: ternarized neural architecture search for resource-constrained edge devices. In *2022 Design, Automation & Test in Europe Conference & Exhibition (DATE)*.

Loni, M., Sinaei, S., Zoljodi, A., Daneshtalab, M., and Sjödin, M. (2020). Deepmaker: A multi-objective optimization framework for deep neural networks in embedded systems. *Microprocessors and Microsystems*, 73.

Loshchilov, I. and Hutter, F. (2017). SGDR: Stochastic gradient descent with warm restarts. In icl (2017). Published online: iclr.cc.

Ma, N., Zhang, X., Liu, M., and Sun, J. (2021). Activate or not: Learning customized activation. In *Proceedings of the International Conference on Computer Vision and Pattern Recognition (CVPR'21)*.

Mocanu, D., Mocanu, E., Stone, P., Nguyen, P., Gibescu, M., and Liotta, A. (2018). Scalable training of artificial neural networks with adaptive sparse connectivity inspired by network science. *Nature Communications*.

Mostafa, H. and Wang, X. (2019). Parameter efficient training of deep convolutional neural networks by dynamic sparse reparameterization. In Chaudhuri and Salakhutdinov (2019).

Mousavi, H., Loni, M., Alibeigi, M., and Daneshtalab, M. (2022). Pr-darts: Pruning-based differentiable architecture search. *CoRR*.

Nair, V. and Hinton, G. E. (2010). Rectified linear units improve restricted boltzmann machines. In Fürnkranz, J. and Joachims, T., editors, *Proceedings of the 27th International Conference on Machine Learning (ICML'10)*. Omnipress.

Nazari, N., Loni, M., Salehi, M., Daneshtalab, M., and Sjödin, M. (2019). Tot-net: An endeavor toward optimizing ternary neural networks. In *2019 22nd Euromicro Conference on Digital System Design (DSD)*.

Ramachandran, P., Zoph, B., and Le, Q. (2018). Searching for activation functions. In *Proceedings of the International Conference on Learning Representations (ICLR'18)*. Published online: iclr.cc.

Sandler, M., Howard, A., Zhu, M., Zhmoginov, A., and Chen, L. (2018). Mobilenetv2: Inverted residuals and linear bottlenecks. In *Proceedings of the International Conference on Computer Vision and Pattern Recognition (CVPR'18)*.

Sehwag, V., Wang, S., Mittal, P., and Jana, S. (2020). Hydra: Pruning adversarially robust neural networks. In Larochelle et al. (2020).

Selman, B. and Gomes, C. (2006). Hill-climbing search. In *Encyclopedia of cognitive science*.

Simonyan, K. and Zisserman, A. (2014). Very deep convolutional networks for large-scale image recognition. *arXiv:1409.1556 [cs.CV]*.

Srinivas, S., Subramanya, A., and Babu, R. (2017). Training sparse neural networks. In *IEEE Conference on Computer Vision and Pattern Recognition Workshops, CVPR Workshops 2017, Honolulu, HI, USA, July 21-26*.

Subramanian, M., Lv, N. P., and VE, S. (2022). Hyperparameter optimization for transfer learning of vgg16 for disease identification in corn leaves using bayesian optimization. *Big Data*, 10.

Sycara, K., Honavar, V., and Spaan, M., editors (2022). *Proceedings of the Thirty-Sixth Conference on Artificial Intelligence (AAAI'22)*. Association for the Advancement of Artificial Intelligence, AAAI Press.

Tanaka, H., Kunin, D., Yamins, D. L., and Ganguli, S. (2020). Pruning neural networks without any data by iteratively conserving synaptic flow. In Larochelle et al. (2020).

Tavakoli, M., Agostinelli, F., and Baldi, P. (2021). Splash: Learnable activation functions for improving accuracy and adversarial robustness. *Neural Networks*.

Tessera, K., Hooker, S., and Rosman, B. (2021). Keep the gradients flowing: Using gradient flow to study sparse network optimization. *CoRR*.

Vischer, M., Lange, R., and Sprekeler, H. (2022). On lottery tickets and minimal task representations in deep reinforcement learning. In *Proceedings of the International Conference on Learning Representations (ICLR'22)*. Published online: `iclr.cc`.

Wallach, H., Larochelle, H., Beygelzimer, A., d'Alché-Buc, F., Fox, E., and Garnett, R., editors (2019). *Proceedings of the 32nd International Conference on Advances in Neural Information Processing Systems (NeurIPS'19)*.

Zamora, J., Rhodes, A. D., and Nachman, L. (2022). Fractional adaptive linear units. In Sycara et al. (2022).

Zhan, H. and Cao, Y. (2019). Deep model compression via deep reinforcement learning. *CoRR*.

Zhou, A., Yao, A., Guo, Y., Xu, L., and Chen, Y. (2017). Incremental network quantization: Towards lossless cnns with low-precision weights. In icl (2017). Published online: `iclr.cc`.

Zhou, H., Lan, J., Liu, R., and Yosinski, J. (2019). Deconstructing lottery tickets: Zeros, signs, and the supermask. In Wallach et al. (2019).

Zhou, Y., Li, D., Huo, S., and Kung, S. (2020). Soft-root-sign activation function. *CoRR*.

Zimmer, L., Lindauer, M., and Hutter, F. (2021). Auto-PyTorch Tabular: Multi-Fidelity MetaLearning for Efficient and Robust AutoDL. *IEEE Transactions on Pattern Analysis and Machine Intelligence*, 43:3079–3090.

A Evaluation of Various Search Algorithms

Figure 6 shows the trend of search performance for finding the best unary operators (Equation (5)) over popular search algorithms, including Late-Acceptance-Hill-Climbing (LAHC), Simulated Annealing (SA), Random Search (RS), and Bayesian Optimization (BO). VGG-16 is trained on CIFAR-10 with a 99% pruning ratio. The bold line represents the mean across three random seeds, while the shaded area represents the confidence intervals. Overall, the observation is that SAFS's search algorithm, LAHC, finds better activation functions than other counterparts with an equal search budget.

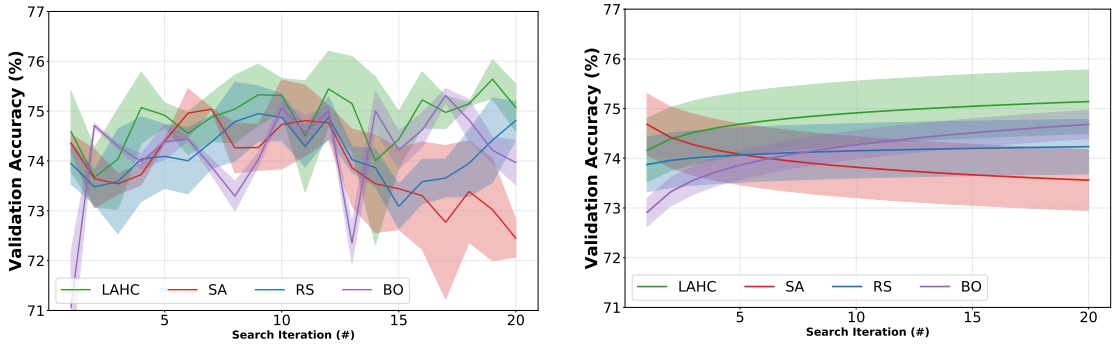

(a) Plotting Search Objective (Vali. Acc.) per Iteration (b) Search Trend

Figure 6: Comparison of different search algorithms (LAHC, SA, RS, BO) for finding the best unary operators for sparse VGG-16 with 99% pruning ratio trained on CIFAR-10. The bold line represents the mean across three random seeds, while the shaded area represents the confidence intervals. (a) Showing raw data. (b) Using a smoothing average function (logarithmic) for representing the trend of data.

B Reporting the Computing Cost of SAFS

Table 3 compares the computing cost (GPU hours) of refining a sparse neural network with SAFS and default vanilla pruning. Although SAFS is slower than the vanilla pruning method, we need to pay this cost only once. Our results show that the significant improvements achieved by SAFS are worth paying this cost. It is important to note that we have not used any multi-fidelity techniques to speed up the first search stage, which is one reason for our slow speed. The use of search acceleration techniques will be explored in the future.

Table 3: Reporting the required computing cost for learning sparse neural network activation functions.

Network	Dataset	GPU Hours (without considering dense training and sparsification)	
		SAFS (with three-fold cross-validation)	Vanilla Pruning (with one-fold cross-validation)
LeNet-5	MNIST	6.4	0.16
VGG-16	CIFAR-10	47	3.8
ResNet-18	CIFAR-10	63	5.6
EfficientNet-B0	ImageNet-16	400	7.7

C Comparison of Accuracy-Compression Ratio Trade-off with State-of-the-Art

We study the effectiveness of SAFS in comparison with various state-of-the-art sparsification and quantization methods in the context of a trade-off between compression ratio (*x-axis*) and performance improvement (*y-axis*) compared to each method's baseline (Figure 7). We examine VGG-16 and ResNet-18 networks trained on CIFAR-10. Our results reveal that SAFS provides 6.24%

higher accuracy and 2.18× more compression ratio for VGG-16 over the best counterparts. SAFS achieves 2.42% higher accuracy than the best counterparts with similar compression ratios for ResNet-18.

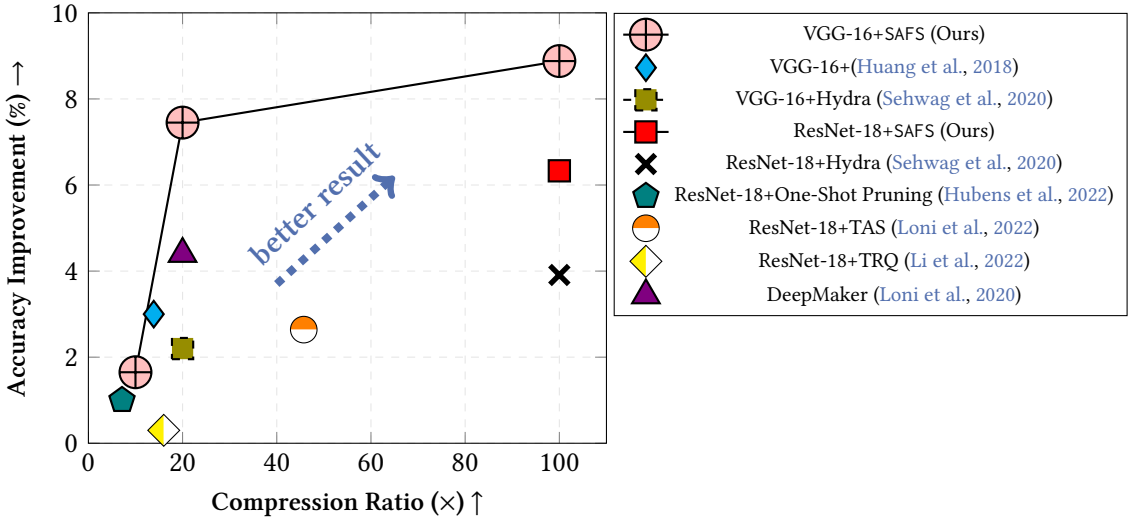

Figure 7: Showing the accuracy improvement (%) vs. the number of network parameters (#Params) of various compact networks trained on CIFAR-10.

D Statement of Reproducibility

To foster reproducibility we address the following points:

Reproducibility analysis. Many works on AutoML have issues regarding reproducibility due to intrinsic stochasticity. To guarantee the reproducibility of results, we follow the Reproducibility checklist proposed by Lindauer and Hutter (2020) (Section 8).

Code release. SAFS is an open-source project. Code is made available through anon-github.automl.cc/r/SAFS-B67D.

Availability of database. In this study, we evaluated our networks using CIFAR-10 (Krizhevsky et al., 2009) and ImageNet-16 (Chrabaszcz et al., 2017) datasets. Thus, this work does not involve any new data collection or human subject evaluation.

Sustainability Analysis. The search process takes up to ≈47 GPU hours for VGG-16 trained on CIFAR-10 on a single NVIDIA® RTX A4000 that produces 2.83 Kg CO_2.

E Details on Searching Networks

Table 4 shows the configuration details of Stage 1 and Stage 2 learning procedures.

Table 5 provides the configuration details for training the dense LeNet-5 model (baseline) with ReLU activation functions trained on MNIST.

Table 6 provides the configuration details for training dense models (baseline) with ReLU activation functions trained on CIFAR-10.

Table 7 provides the configuration details for training dense models (baseline) with ReLU activation functions trained on ImageNet-16.

Table 8 presents specifications of hardware devices utilized for evaluating the performance of SAFS.

Table 4: Table showing the general hyperparameter configuration for SAFS learning procedures.

Stage 1: Learning Unary Operators	
Unary Operators[∓]	ReLU6 (Howard et al., 2017), Acon (Ma et al., 2021), TanhSoft-1 (Biswas et al., 2021) SRS (Zhou et al., 2020), Symlog (Hafner et al., 2023), Symexp (Hafner et al., 2023) Swish, Tanh, HardSwish, ELU, GELU, Softplus, LogisticSigmoid
History Length	3
Number of Iterations	20
Epochs for Evaluation	80
Stage 2: Scaling factors and HPO	
HPO Library	SMAC3[*]
Learning Rate	$1e^{-4} < lr < 1e^{-1}$
Learning Rate Scheduler	*constant, step, linear, cosine annealing (Loshchilov and Hutter, 2017)* $\{0.001 \times (0.5^{epoch\%20})\}$, *ReduceLROnPlateau*[†], *CosineAnnealingWarmRestarts*[‡]
Optimizer	SGD, Adam, Fromage, TAdam (Ilboudo et al., 2020)

[∓] (Dubey et al., 2022) explains in detail popular activation functions considered in this study.
[*] https://github.com/automl/SMAC3
[†] https://pytorch.org/docs/stable/generated/torch.optim.lr_scheduler.ReduceLROnPlateau.html
[‡] https://pytorch.org/docs/stable/generated/torch.optim.lr_scheduler.CosineAnnealingWarmRestarts.html

Table 5: Dense CNNs with training hyperparameters for MNIST dataset used in experiments.

Network[‡]	LeNet-5
Epoch (#)	100
Learning Rate (lr)	0.1
Learning Rate Scheduler	None
Optimizer	SGD
Train Time (GPU Hours) for One Model (One-fold)	0.16

[‡] Original implementation of dense model: https://github.com/ChawDoe/LeNet5-MNIST-PyTorch/blob/master/train.py

Table 6: Dense CNNs with training hyperparameters for CIFAR-10 dataset used in experiments.

Network	VGG-16	ResNet-18
Epoch (#)	200	200
Learning Rate (lr)	0.001	0.01
Learning Rate Scheduler	$0.001 \times (0.5^{epoch\%20})$	*ReduceLROnPlateau*[‡]: {factor: 0.05, patience: 2, min_lr: 0, threshold: 0.0001, eps:$1e^{-8}$ }
Weight Decay	$5e^{-4}$	$5e^{-4}$
Momentum	0.9	0.9
Optimizer	SGD	SGD
Train Time (GPU Hours) for One Model (One-fold)	1.25	4.0

[‡] https://pytorch.org/docs/stable/generated/torch.optim.lr_scheduler.ReduceLROnPlateau.html

Table 7: Dense CNNs with training hyperparameters for ImageNet-16 dataset used in experiments.

Network	EfficientNet-B0	ResNet-18
Epoch (#)	50	50
Learning Rate (lr)	0.01	0.1
Learning Rate Scheduler	*CosineAnnealingWarmRestarts*[‡]: {#Iterations for first restart: 12, Minimum learning rate:$5e^{-5}$ }	*CosineAnnealingWarmRestarts*[‡]: {#Iterations for first restart: 12, Minimum learning rate:$5e^{-5}$ }
Weight Decay	$5e^{-4}$	$5e^{-4}$
Momentum	0.9	0.9
Optimizer	SGD	SGD
Train Time (GPU Hours) for One Model (One-fold)	18	16

[‡] https://pytorch.org/docs/stable/generated/torch.optim.lr_scheduler.CosineAnnealingWarmRestarts.html

Table 8: Hardware Specification for search & train.

Parameter	Specification
GPU	NVIDIA® RTX A4000 (735 MHz)
GPU Memory	16 GB GDDR6
GPU Compiler	cuDNN version 11.1
System Memory	64 GB
Operating System	Ubuntu 18.04
CO_2 Emission/Day †	1.45 Kg
† Calculated using the ML CO_2 impact framework (Lacoste et al., 2019).	